Viologen-functionalized single-walled carbon nanotubes as carrier nanotags for electrochemical immunosensing. Application to TGF-β1 cytokine

Esther Sánchez-Tirado, Luis M. Arellano, Araceli González-Cortés, Paloma Yáñez-Sedeño, Fernando Langa, José M. Pingarrón

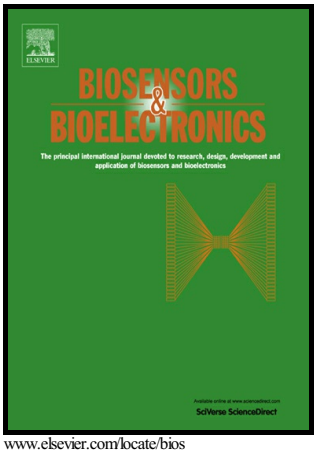

www.elsevier.com/locate/bios

PII: S0956-5663(17)30448-7
DOI: http://dx.doi.org/10.1016/j.bios.2017.06.063
Reference: BIOS9833

To appear in: *Biosensors and Bioelectronic*

Received date: 12 April 2017
Revised date: 19 June 2017
Accepted date: 30 June 2017

Cite this article as: Esther Sánchez-Tirado, Luis M. Arellano, Araceli González-Cortés, Paloma Yáñez-Sedeño, Fernando Langa and José M. Pingarrón, Viologen-functionalized single-walled carbon nanotubes as carrier nanotags for electrochemical immunosensing. Application to TGF-β1 cytokine, *Biosensors and Bioelectronic,* http://dx.doi.org/10.1016/j.bios.2017.06.063

Viologen-functionalized single-walled carbon nanotubes as carrier nanotags for electrochemical immunosensing. Application to TGF-β1 cytokine

Esther Sánchez-Tirado[a], Luis M. Arellano[a,b], Araceli González-Cortés[a], Paloma Yáñez-Sedeño[a*], Fernando Langa[a,b*], José M. Pingarrón[a]

[a]Department of Analytical Chemistry, Faculty of Chemistry, University Complutense of Madrid, Ciudad Universitaria s/n, 28040-Madrid, Spain;
[b]Instituto de Nanociencia, Nanotecnología y Materiales Moleculares (INAMOL), Universidad de Castilla-La Mancha, 45071-Toledo, Spain

yseo@quim.ucm.es
Fernando.Langa@uclm.es
[*]Corresponding authors.

Abstract: Viologen-SWCNT hybrids are synthesized by aryl-diazonium chemistry in the presence of isoamyl nitrite followed by condensation reaction of the resulting HOOC-Phe-SWCNT with 1-(3-aminoethyl)-4,4'-bipyridinium bromine and N-alkylation with 2-bromoethylamine. The V-Phe-SWCNT hybrids were characterized by using different spectroscopic techniques (FT-IR, Raman, UV-vis), TGA and Kaiser test. Viologen-SWCNTs were used for the preparation of an electrochemical immunosensor for the determination of the transforming growth factor β1 (TGF-β1) cytokine considered as a reliable biomarker in several human diseases. The methodology involved preparation of V-Phe-SWCNT(-HRP)-anti-TGF conjugates by covalent linkage of HRP and anti-TGF onto V-Phe-SWCNT hybrids. Biotinylated anti-TGF antibodies were immobilized onto 4-carboxyphenyl-functionalized SPCEs modified with streptavidin and a sandwich type

immunoassay was implemented for TGF-β1 with signal amplification using V-Phe-SWCNT(-HRP)-anti-TGF conjugates as carrier tags. The analytical characteristics exhibited by the as prepared immunosensor (range of linearity between 2.5 and 1000 pg mL^{-1} TGF-β1; detection limit of 0.95 pg mL^{-1}) improve notably those reported with other previous immunosensors or ELISA kits. A great selectivity against other proteins was also found. The prepared immunosensor was validated by determining TGF-β1 in real saliva samples. Minimal sample treatment was required and the obtained results were in excellent agreement with those obtained by using a commercial ELISA kit.

Keywords: viologen, transforming growth factor β1, cytokine, saliva, electrochemical immunosensor

1. Introduction

Viologens are 4,4´-bipyridine derivatives which exhibit reversible electrochemical responses at negative potentials corresponding to their three possible oxidation states, $V^{2+} \leftrightarrow V^{+\cdot} \leftrightarrow V^{0}$. The first reaction constitutes the basis for application of viologens as electron acceptors and electron transfer mediators to various proteins [Chen et al., 2009]. The reversible redox behavior promotes the electron exchange between electrodes and proteins with the subsequent decrease in the ohmic overpotential [Lee et al., 2016]. Taking advantage of this behavior, various electrochemical biosensors based on the use of viologens have been described. However, due to the solubility of viologen cations in aqueous solution and their high toxicity, immobilization on electrode surfaces using different strategies and materials is usually performed [Lee et al., 2016] [Ghica et al., 2005]. An illustrative example of strategy not involving physical entrapment of viologen is the modification of a GCE based on the amino radical oxidation with subsequent formation

of a carbon-nitrogen linkage on the electrode for the preparation of a hydrogen peroxide biosensor with horseradish peroxidase and gold nanoparticles [Jia et al., 2008]. . Another interesting approach relies on modification of a gold electrode with a self-assembled monolayer of thiol-functionalized viologen which was used to design a biosensor involving direct electron transfer of hemoglobin for the detection of H_2O_2 [Kafi et al., 2007].

Configurations using viologens have been implemented in the development of electrochemical immunosensors. A label-free design for the detection of α-fetoprotein was reported using gold nanoparticles functionalized by covalent surface capping with 1,1′-bis-(2-mercapto)-4,4′-bipyridinium dibromide [Liang et al., 2009]. A platform for the construction of multi-array electrochemical immunosensors was prepared by immobilization of biotinylated viologen on modified polypyrrole-streptavidin films. In this strategy, the change in the electrochemical response of the redox molecule corresponding to the two electrons reduction of di-cationic to neutral viologen was monitored after the antibody-antigen interaction [Miodek et al., 2016]. The direct impedimetric detection of an anti-cholera toxin antibody was performed by using electropolymerized biotinylated poly(pyrrole-viologen) film as scaffold for the development of reagentless immunosensors [Gondram et al., 2010]. The selective detection of α-fetoprotein (AFP) was performed by using an electrochemical immunosensor prepared by covalent immobilization of polyamidoamine (PAMAM) dendrimer-encapsulated AuNPs on a gold electrode followed by sequential immobilization of ethyleneamine-viologen as the redox marker and AFP antibody [Kavosi et al., 2014]. Regarding DNA sensors, an interesting strategy involved a conjugate integrating an anthracene chromophore and a viologen moiety in the same molecular skeleton for discrimination between non-hybridized and hybridized surface-immobilized DNA [Conoci et al., 2014].

Viologens have been immobilized on materials such as graphene oxide [Park et al., 2012], conductive polymers [Gadgil et al., 2013], dendrimers [Kavosi et al., 2014] and carbon nanotubes (CNTs). Immobilization methods on CNTs included drop casting of viologen solution and electrochemical treatment by cyclic voltammetry [Swetha et al., 2012] [Lee et al., 2016], preparation of multilayers assembled through electrostatic interactions [Wang et al., 2008], and formation of composites [Wang et al., 2009]. Few examples of covalent attachment of viologens on CNTs have been described so far. Synthesis of an asymmetrically substituted viologen covalently anchored to SWCNTs through an ester linkage by reacting chlorinated purified SWCNTs with *N*-methyl-*N´*-(6-hydroxyhexyl)-4,4´-bipyridine was reported [Alvaro et al., 2005]. More recently, Liu et al. [Liu et al., 2013] linked covalently an electroactive organic electrolyte of viologen on MWCNTs through a diazonium coupling process to form layer-by-layer (LBL) multi-layers with poly(sodium-p-styrenesulfonate) at interfaces. A couple of redox waves in the potential range of -0.3 – -0.7 V vs. Ag/AgCl, corresponding to the electron transfer process of MWCNT-PhV^{2+} ↔ MWCNT-PhV$^{+\bullet}$ was observed.

Transforming growth factor β1 (TGF-β1) is a cytokine belonging to the structurally related group of multifunctional TGF-βs which regulates a variety of biological processes. In particular, TGF-β1 is involved in immune and inflammatory responses [Tsapenko et al., 2013] and is considered as a good biomarker of bladder carcinoma, liver fibrosis, or renal diseases. Normal levels of this protein are in the 0.1 - 25 ng/mL range in plasma of healthy individuals [Grainger et al., 2000]. However, noticeable increases in circulating TGF-β1 can be found in patients suffering various types of cancer [Wickenhauser et al., 1995] or autoimmune disorders [Pfeiffer et al., 1996]. Methods for the determination of this cytokine comprise immunoassays with ELISA kits involving sandwich type configurations and

peroxidase-labeled or biotinylated immunoreagents. Regarding electrochemical immunosensors, very few methods can be found in the literature. An impedimetric design for the determination of TGF-β1 in serum was reported involving the preparation of a self-assembled monolayer of polyethylene glycol coated onto interdigitated electrodes. Covalent immobilization of antibodies allowed TGF-β1 determination in a linear range between 1 and 1000 ng/mL with a detection limit of 0.570 ng/mL [Yao et al., 2016]. CNTs functionalized by click chemistry were used as scaffolds for the preparation of an electrochemical immunosensor for TGF-β1 determination in serum [Sánchez-Tirado et al., 2016]. MWCNTs were functionalized by means of copper(I) catalyzed azide–alkyne cycloaddition followed by conjugation of an alkyne-functionalized IgG and assembling IgG-alkyne–azide–MWCNT conjugates for immobilization of antibodies. Once the target cytokine was sandwiched with biotinylated anti-TGF labeled with poly(HRP-Strept) conjugates, the affinity reaction was monitored amperometrically at −0.20 V using the hydroquinone/H_2O_2 system. The calibration plot for TGF-β1 exhibited a range of linearity extending between 5 and 200 pg/mL, and the limit of detection was 1.3 pg/mL. Recently, our group also developed an amperometric immunosensor for TGF-β1 using carboxylic acid-functionalized magnetic microparticles supported onto screen-printed carbon electrodes (SPCEs) to immobilize covalently the specific antibodies by means of Mix&Go polymer. A sandwich-type scheme was prepared with anti-TGF-biotin and conjugation with poly(HRP-Strept) for signal amplification. Amperometric measurements as described above provided a calibration plot with a linear range between 15 and 3000 pg/mL and a LOD value of 10 pg/mL. This configuration was validated by analyzing spiked urine at different TGF-β1 pg/mL concentration levels [Sánchez-Tirado et al., 2017]. Moreover, an aptasensor for TGF-β1 involving aptamer-modified Au electrodes integrated with

microfluidics was reported. Thiolated aptamers labeled with methylene blue were self-assembled on gold surfaces. The linear range covered up to 250 ng/mL with a detection limit of 1ng/mL. This device was used to monitor TGF-β1 release from hepatic cells [Matharu et al., 2014].

This work reports a novel method for the preparation of viologen-SWCNT hybrids (V-Phe-SWCNTs) through aryl-diazonium chemistry in the presence of isoamyl nitrite followed by simple condensation reaction of the resulting HOOC-Phe-SWCNT with 1-(3-aminoethyl)-4,4'-bipyridinium bromine and N-alkylation with 2-bromoethylamine. The as prepared V-Phe-SWCNTs are used as carrier tags for signal amplification in the construction of an amperometric immunosensor for TGF-β1. Anti-TGF antibodies and HRP were immobilized on the synthesized V-Phe-SWCNT hybrids, and the target cytokine was sandwiched with V-Phe-SWCNT(-HRP)-anti-TGF conjugates and biotinylated antibodies immobilized onto SPCEs modified with streptavidin. The implementation of a sandwich type immunoassay allowed improved analytical characteristics to be obtained in terms of wider linear dynamic range of response and lower detection limit than those reported with other immunosensors and ELISA kits. In addition, a great selectivity against other proteins and ascorbic and uric acid was also found. The developed immunosensor was validated by determining TGF-β1 in real saliva samples with minimal sample treatment, and providing results in excellent agreement with those obtained by using a commercial ELISA kit.

2. Experimental

2.1. Reagents and solutions.

All commercial solvents and reagents used for the synthesis of V-Phe-SWCNTs were employed without further purification. HiPco SWCNTs were purchased from NanoIntegris (www.nanointegris.com), with a diameter between 0.8-1.2 nm and length 100-1000 nm. Chicken biotinylated antibody (anti-TGF-Biotin), human TGF–β1, and mouse antibody (anti-TGF) were from R&D Systems. These reagents were included in the Duo Sets ELISA Development System (DY240-05). Horseradish peroxidase (HRP), streptavidin, hydrogen peroxide, hydroquinone, and terephthalic acid were from Sigma. 1–ethyl–3–(3–dimethylaminopropyl)carbodiimide(EDC),*N*–hydroxy-sulfosuccinimide (NHSS), and 4-aminobenzoic acid (4-ABA) were from Across. Sodium nitrite from Panreac was also used. Anti-TGF-Biotin solutions were prepared in Reagent Diluent 1 from Duoset® Ancillary Reagent Kit 1 (R&D Systems, DY007). Anti-TGF solutions were prepared in 0.1 M phosphate buffer solution of pH 7.4. This buffer solution was also used for preparing 0.5 mM solutions of D-biotin (Gerbu) used as blocking agent. 25 mM MES buffer solution of pH 5.0 prepared from 2–(N–morpholine) ethanosulfonic acid (Gerbu) was also used. Adiponectin (APN), tumor necrosis factor alfa (TNF–α) and interleukin 1 beta (IL–1β) from R&D Systems, cortisol and human inmunoglobulin G (IgG) from Sigma,interleukin 6 (IL–6) and interleukin 8 (IL–8) from Abcam, and bovine serum albumin (BSA, Gerbu) were tested as potential interfering compounds. Deionized water was obtained from a Millipore Milli-Q purification system (18.2M Ω cm at 25 °C).

2.2. Apparatus and electrodes.

Nuclear magnetic resonance 1H and 13C were recorded using Bruker Innova 400 MHz. Absorption spectra (UV-vis) were performed on Shimadzu UV 3600 spectrophotometer.

The thermogravimetric analysis was performed on a Mettler Toledo TGA/DSC Linea Excellent under inert atmosphere of nitrogen with a rate of 10°C/min, and the weight changes were recorded as a function of temperature. Raman measurements were carried out with a Renishaw inVia Reflex Confocal Raman Microscope at room temperature using laser excitation of 785 nm. Measurements were taken with 10 s of exposure times at varying numbers of accumulations. The laser spot was focused on the sample surface using a long working distance 100x objective. Raman spectra were collected on numerous spots on the sample and recorded with a Peltier cooled CCD camera. The sample was measured on glass without any sample preparation. The intensity ratio ID/IG was obtained by taking the peak intensities following any baseline corrections. FTIR spectrum were obtained on Avatar 370 Thermo Nicolet spectrophotometer using KBr pellets.

The following instruments were utilized for the preparation and functioning of the immunosensor: An INBEA potentiostat provided with the Ib Graph software was used for the amperometric measurements; electrochemical impedance spectroscopy was carried out with a μAutolab type III potentiostat (Ecochemie) controlled by FRA2 software. Screen-printed carbon electrodes (SPCEs, 110 DRP, ϕ 4 mm) purchased from DropSens (Oviedo, Spain) were used as working electrodes. These electrodes were provided with a silver pseudo-reference electrode and a carbon counter electrode. A Crison Basic 20+ pHmeter, an Elmasonic S-60 ultrasonic bath (Elma), an MPW-65R centrifuge from MPW Med. Instruments, a Vortex homogenizer and a magnetic stirrer, both from Velp Scientifica, were also employed.

2.3. Procedures

2.3.1. Functionalization of SWCNT.

The preparation of viologen-SWCNT hybrid (V-Phe-SWCNT) was performed in three steps:

1. Synthesis of 1-(3-aminoethyl)-4,4'-bipyridinium bromine: A solution of 4,4'-bipyridine (500 mg, 3.2 mmol) and 2-bromoethylamine (71.4 mg, 0.32 mmol) in acetonitrile (10 mL) was refluxed for 1.5 h. After cooling, the precipitate was filtered and re-dissolved in hot DMF to remove the di-alkylated salt by filtration. In order to get the mono-alkylated product as a white solid, diethyl ether was added. Yield: 59 %. ^{1}H NMR (400 MHz, D_2O); δ: 9.08 (d, *J* = 6.3 Hz, 2H), 8.80 (d, 2H), 8.52 (d, *J* = 6.3 Hz, 2H), 7.95 (d, *J* = 6.3 Hz, 2H), 5.06 (t, *J* = 6.5 Hz, 2H), 3.78 (t, *J* = 6.5 Hz, 2H).^{13}C NMR (100 MHz, D_2O); δ: 155.11, 149.91, 145.35, 142.31, 126.62, 122.54, 57.63, 39.11.

2. Synthesis of HOOC-SWCNT: A suspension of pristine-SWCNT (20 mg) in *N*-methyl-2-pyrrolidone (40 mL) was sonicated for 10 min, then 4-aminobenzoic acid (457 mg, 3.33 mmol, and isoamyl nitrite (0.54 mL, 3.98 mmol) were added. The mixture was stirred under argon atmosphere at 70°C for 24 h. After cooling, the crude was filtered through PTFE membrane (Millipore 0.1 μm pore) and washed subsequently with NMP, MeOH and CH_2Cl_2, until the filtrate was clear, to obtain the carbon-based material as a black solid (23 mg).

3. Synthesis of viologen-SWCNT hybrid (V-Phe-SWCNT): SWCNT-Phe-COOH (8 mg) were dispersed in DMF anhydrous (20 mL) *N*,*N'*-dicyclohexylcarbodiimide (DCC) (21.9 mg, 0.11 mmol), hydroxybenzotriazole (HOBt) (14.4 mg, 0.11 mmol), and 1-(3-aminoethyl)-4,4'-bipyridinium bromine (16 mg, 0.08 mmol) were added to the mixture under argon atmosphere. The suspension was sonicated for 10 minutes and heated at 60°C for 3 days. The solid was separated by filtration through a PFTE membrane (Millipore 0.1

μm pore) and washed several times with hot DMF, MeOH and CH_2Cl_2. Thereafter, the solid was re-dissolved in DMF, and 2-bromoethylamine (16 mg, 0.08 mmol) was added. The reaction mixture was heated at 120°C for 24 h, and then filtered on a PFTE membrane (Millipore 0.1 μm pore). Finally, the solid was washed with DMF, MeOH and CH_2Cl_2 to get the V-Phe-SWCNTs (9.4 mg).

2.3.2. Preparation of V-Phe-SWCNT(-HRP)-anti-TGF conjugate.

To obtain 100 μL of V-Phe-SWCNT(-HRP)-anti-TGF, 50 μL of a 200 mM EDC/NHSS solution prepared in 25 mM MES of pH 5.0 were mixed with 50 μL of 4 mg mL^{-1} terephthalic acid, and 100 μL of each 40 μg mL^{-1} HRP, 4 μg mL^{-1} anti–TGF. and 0.5 mg mL^{-1} aqueous V–SWCNT suspension. The mixture was incubated under magnetic stirring in the dark for 3 h. Once centrifuged at 8^{o}C and 14,000 rpm for 10 min, supernatant was retired and two washing steps with 500 μL of 0.1 M PBS of pH 7.4 were performed. Finally, the obtained conjugate was suspended in 100 μL of PBS.

2.3.3. Preparation of V-Phe-SWCNT(-HRP)-anti-TGF-TGF-β1-anti-TGF-Biotin-Strept/ SPCEs.

In a first step, SPCEs were modified by grafting of a 4-ABA diazonium salt on the electrode surface. In order to do that, 20 mg of 4-ABA were dissolved in 2 mL of 1 M HCl and cooled with ice. Then, the diazonium salt was prepared by adding 2 mM $NaNO_2$ aqueous solution dropwise to this solution (38 μL for each 200 μL) with constant stirring. Next, 40 μL of the resulting solution was casted onto the SPCE and ten successive cyclic voltammetric scans between 0.0 and −1.0 V (ν = 200 mV s^{-1}) were carried out. The modified electrodes were washed thoroughly with water and dried at room temperature. Dried ABA-g-SPCEs were activated by dropping 5 μL of EDC/NHSS (0.1 M each) prepared in MES buffer solution of pH 5.0 and allowed 30 min to stand. After rinsing with

water, 5 µL of a 200 µg mL^{-1} streptavidin solution prepared in MES buffer of pH 5.0 were added and left to react for 1 h. Next, the electrodes were rinsed with water and dried. Immobilization of biotinylated antibody was further performed by adding 5 µL of a 7.5 µg mL^{-1} anti-TGF-Biotin prepared in Reagent Diluent 1 from Duoset® Ancillary Reagent Kit 1 (R&D Systems, DY007) on the modified electrode and left to stand for 60 min. Then, a blocking step was made by adding 5 µL of a 0.5 mg mL^{-1} biotin and left to incubate 30 min. Thereafter, 5 µL of standard TGF–β1 solutions or the samples were placed onto the electrode surface and incubated for 60 min. After washing with water and drying, 5 µL of V–SWCNT(-HRP)-anti-TGF were dropped onto the electrode and incubated for 60 min. Finally, the immunosensor was washed again and maintained with a drop of a 0.05 M PBS solution of pH 6.0 until the measurements were made.

2.3.4. Amperometric measurements.

Amperometric measurements were performed by adding 45 µL of 0.5 M PBS of pH 6.0 to the immunosensor surface and applying a potential of -300 mV. Once the background current was stabilized, (around 100 s), 5 µL of 50 mM H_2O_2 were added and allowed standing for 200 s to complete the enzyme reaction.

2.3.5. Analysis of saliva.

Saliva samples were obtained from volunteers and collected using a Salivette® collection device (Sarstedt). Briefly, once rinsed the mouth thoroughly with water, a cotton swab was inserted into the mouth and chewed for 1 min. Then, the swap saturated with saliva was inserted into the vial, sealed with the cap and centrifuged for 10 min at 3000 rpm. The determination was performed immediately by applying the procedure described above to 5 µL of undiluted saliva and interpolation of the amperometric response in the calibration plot constructed with standard solutions.

3. Results and discussion

The synthesis of V-Phe-SWCNT hybrids was accomplished by following the procedure described in the Experimental section according with the Scheme 1. Briefly, careful mono-alkylation of viologen with 2-bromoethylamine in stoichiometric conditions afforded 1-(3-aminoethyl)-4,4'-bipyridinium bromine; functionalization of SWCNT was based on well-known aryl-diazonium chemistry in the presence of isoamyl nitrite [Palacin et al., 2009] followed by simple condensation reaction of the resulting HOOC-Phe-SWCNT with 1-(3-aminoethyl)-4,4'-bipyridinium bromine.

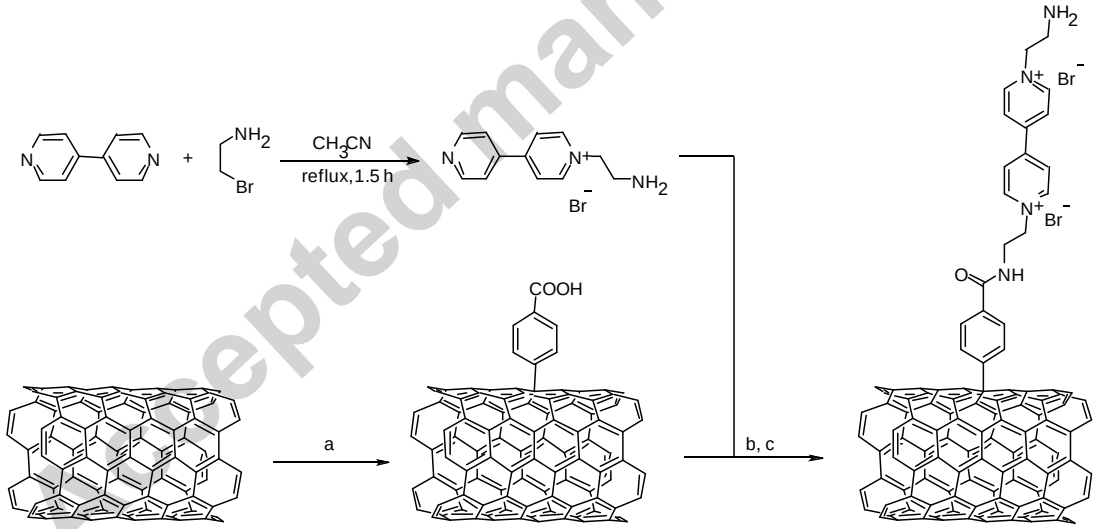

Scheme 1. Scheme showing the steps for the synthesis of V-Phe-SWCNTs. Reagents and conditions: (a) 4-aminobenzoic acid, isoamylnitrite, NMP, 70°C for 24h; (b) *1*-(3-aminoethyl)-4,4'-bipyridinium bromine, DCC, HOBt, at 60°C, 3 days; (c) 2-bromoethylamine, DMF, 120°C, 24 h.

The V-Phe-SWCNT hybrids were characterized by using different spectroscopic techniques (FT-IR, Raman, UV-vis spectroscopies), TGA and Kaiser test. Details on this characterization are given in the Supplementary Material.

The functionalization degree of SWCNT hybrids and the amount of groups anchored to the nanotubes were quantified by TGA. Samples were heated over a temperature range of 40 - 1000 ºC at a scanning rate of 10ºC/min under nitrogen atmosphere. At 600°C, the thermogram shown in Figure S1 shows a weight loss of 10.3 % for *pristine*-SWCNT, 24.4 % for HOOC-Phe-SWCNT and 43.6 % for V-Phe-SWCNT. The corrected weight loss due to the functional groups on CNTs was estimated to be 14 % for HOOC-Phe-SWCNT and 33.3 % for V-Phe-SWCNT. Consequently, the number of phenyl acid functional groups in SWCNT was estimated as 1 per 50 carbon atoms, and with the same calculation, the number of viologen groups attached to the sidewall is approximately 1 per 114 carbon atoms.

Raman spectra (Figure 1) of *pristine*-SWCNT showed the characteristics bands, a disorder mode (D-Band) with low intensity at 1292 cm^{-1} and a tangential mode (G-Band) at 1595 cm^{-1}(I_D/I_G =0.09). After functionalization, the intensity of the D-Band (I_D/I_G =0.54) increased (associated with the transformation of the sp^2 to sp^3 carbons), which indicated the incorporation of organic moiety on the surface of the CNT. Figure S2(A) shows the radial breathing mode of the CNT (RBM zone) before and after Tour reaction. The reduction of the tubes intensity also confirms the incorporation of the different species on the wall. Furthermore, the G^+-Band is sensitive to charge transfer, as shown at Figure S2(B), the G-Band is up-shifted by 2 cm^{-1} in the V-Phe-SWCNT as compared to *pristine*-SWCNT due to

the p-doping [Straub et al., 2014] [Voggu et al., 2008]. This result confirmed that the electron-acceptor viologen was attached on the skeleton of SWCNT.

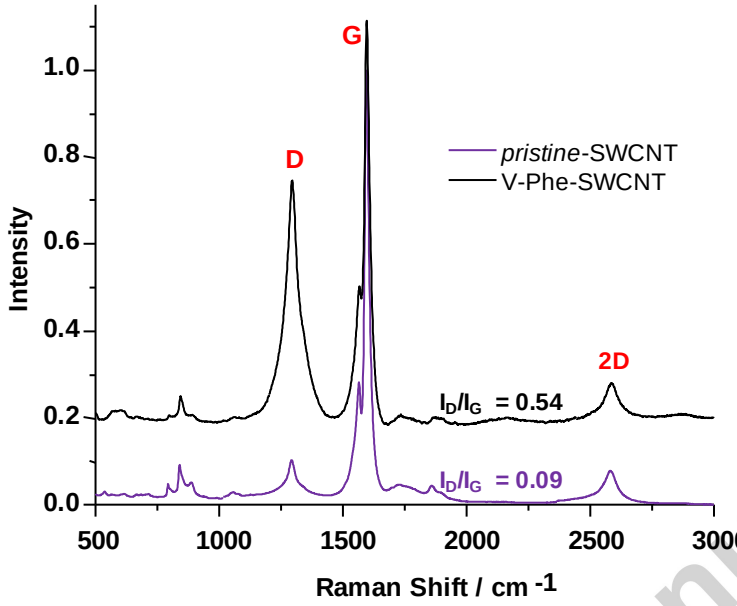

Figure 1. Raman spectra (785 nm excitation) of *pristine*-SWCNT and V-Phe-SWCNT. The relative degree of functionalization was calculated by dividing the intensity of the D-Band by the G-Band.

FT-IR spectroscopy provided important information about the covalent linkage of the viologen on the surface of SWCNT (Figure S3). Comparing with *pristine*-SWCNT, V-Phe-SWCNT showed the characteristic bands of the skeletal in-plane vibrations of graphitic domains at 1554 cm^{-1}, the aliphatic C-H stretching mode at 2919 $cm^{-1}$and aromatic C-H nearby 3005 cm^{-1}. Furthermore, the appearance of strong peaks attributed to the viologen units were clearly observed at 3450 cm^{-1} (2x N-H vibrations), and 1095 cm^{-1} (C-N bond). In addition, a new peak at 1642 cm^{-1} was observed which can be assigned to an amide carbonyl stretching mode indicating the chemical attachment of the viologen on the

SWCNT wall. In agreement with Raman and FT-IR information, UV-vis spectra of the V-Phe-SWCNT hybrid (Figure S4) revealed the presence of the viologen unit by the appearance of a peak at 382 nm conversely to that observed with the *pristine*-SWCNT. The presence of primary amine on the V-Phe-SWCNT hybrid was determined by using the Kaiser test [Tuci et al., 2012].

Preparation of the V-Phe-SWCNT(-HRP)-anti-TGF-TGF-β1-anti-TGF-Biotin-Strept/ SPCE immunosensor.

The methodology employed for the preparation of the immunosensor involved the following steps: a) preparation of V-Phe-SWCNT(-HRP)-anti-TGF conjugates by covalent linkage of HRP and anti-TGF onto V-Phe-SWCNT hybrids; b) construction of the immunosensing platform by immobilizing biotinylated antibodies onto 4-carboxyphenyl-functionalized SPCEs modified with covalently bonded streptavidin; c) implementation of a sandwich type immunoassay for TGF-β1 with signal amplification through the use of V-Phe-SWCNT(-HRP)-anti-TGF conjugates as carrier tags. The protocols used were described in the Experimental section, and Figure 2 shows schematically these steps and the reaction providing the electrochemical response. The proposed strategy took advantage of both the good performance of grafted electrochemical scaffolds for covalent immobilization of immunoreagents, and the amplification of the electrochemical responses with V-Phe-SWCNT(-HRP)-anti-TGF conjugates. Modification of carbon electrodes through free radical grafting is known to provide compact and stable monolayers with specific functionalities. In the followed method, the electrochemical reduction of diazonium salt of 4-ABA onto SPCEs was performed followed by streptavidin immobilization by means of

EDC/NHSS chemistry. The experimental conditions used in this step were those optimized previously [Moreno-Guzmán et al., 2012].

Regarding V-Phe-SWCNT(-HRP)-anti-TGF conjugates used as signals amplification tags, they were prepared by covalent immobilization of HRP and anti-TGF on the V-Phe-SWCNTs. In order to attain the maximum number of biomolecules immobilized on the nanotubes conjugate, covalent attachment to carboxylic groups at HOOC-Phe-SWCNTs was performed after activation with EDC/NHSS system and, furthermore, terephthalic acid was used as carbonyl-terminated linker for covalently immobilization onto amino groups of viologen moiety [Rahim Ruslinda et al., 2013].

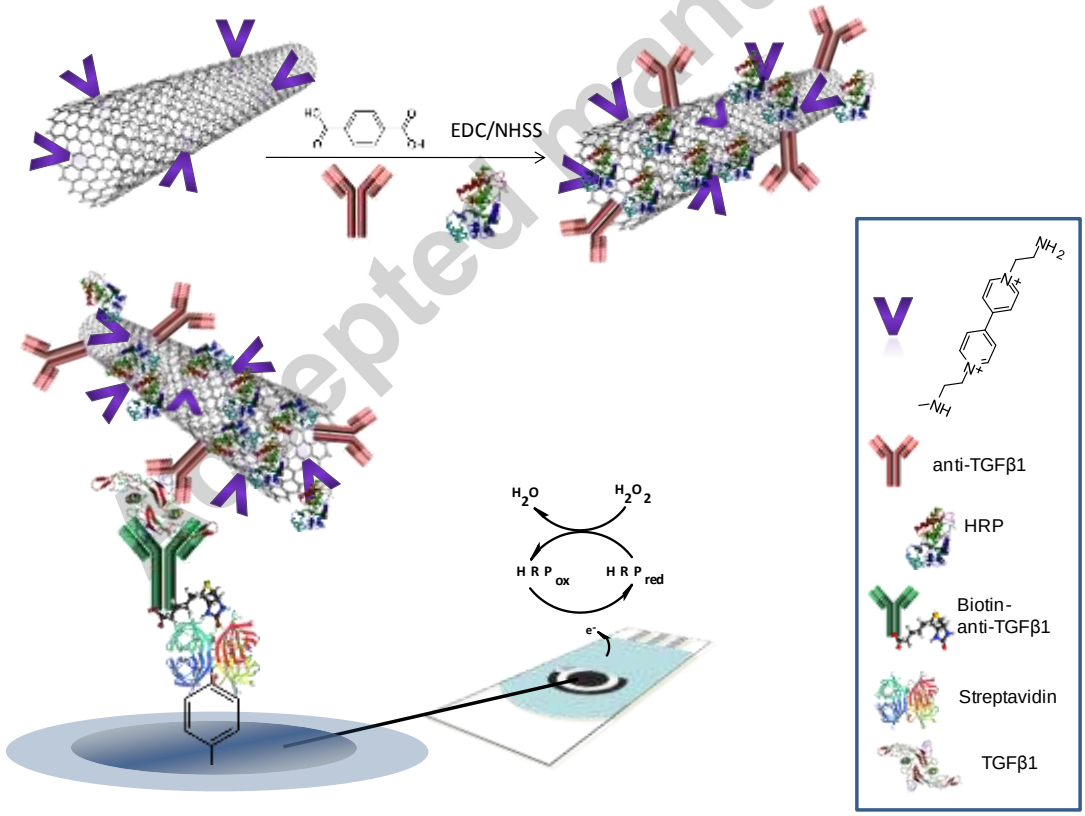

Figure 2. Schematic display of the different steps involved in the construction of an amperometric immunosensor for TGF-β1 using V-Phe-SWCNT hybrids

Characterization of V-Phe-SWCNT(-HRP)-anti-TGF by UV-vis and FT-IR spectroscopies was also made with the results showed in the Supplementary Material (Figure S5). Absorption spectra of V-Phe-SWCNT(-HRP)-anti-TGF shows the band at 266 nm corresponding to the presence of the antibody (see Figure S5A), which confirmed the successful formation of the hybrid. Regarding FT-IR spectrum of V-Phe-SWCNT-HRP-anti-TGF (Figure S5B) it showed a broader band for the characteristic O-H bending vibration at 3429 cm^{-1}, besides to new bands in the fingerprint region, which confirmed the antibody attachment, while the characteristic bands of V-SWCNT-Phe were maintained. In addition, V-Phe-SWCNT(-HRP)-anti-TGF displayed new bands at 803 cm^{-1}, around 656 cm^{-1} and 478 cm^{-1}, which are associated with the bound of antibody.

Figure 3 shows cyclic voltammograms recorded in the 0.0 to -0.8 V potential range (vs. Ag pseudo-reference electrode) at V-Phe-SWCNT/GCE (curves 1 and 3) and V-Phe-SWCNT-HRP/GCE (curves 2 and 4) for solutions prepared in absence and in the presence of H_2O_2. As expected, the V-Phe-SWCNT-HRP/SPCE provided more sensitive response to the reduction of H_2O_2 which can be attributed to the role of V-Phe-SWCNT as mediator of the HRP catalytic reaction [Dong et al., 1997]. This behavior is in agreement with that reported by Jia[5] for the electrochemical reduction of H_2O_2 at a glassy carbon electrode modified with gold nanoparticles-N,N′-bis(3-aminopropyl-4,4′-bipyridinium) tetrabromide (AuNPs/ BAPV/GCE) in the absence and in the presence of HRP. The following reaction scheme was suggested for the electrocatalytic process [Quan et al., 2010].

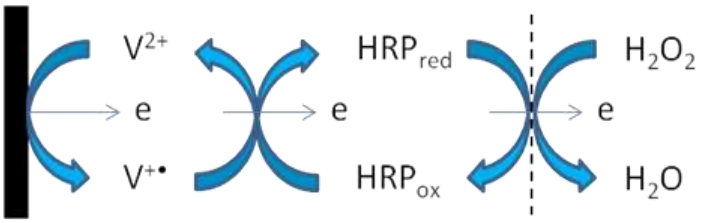

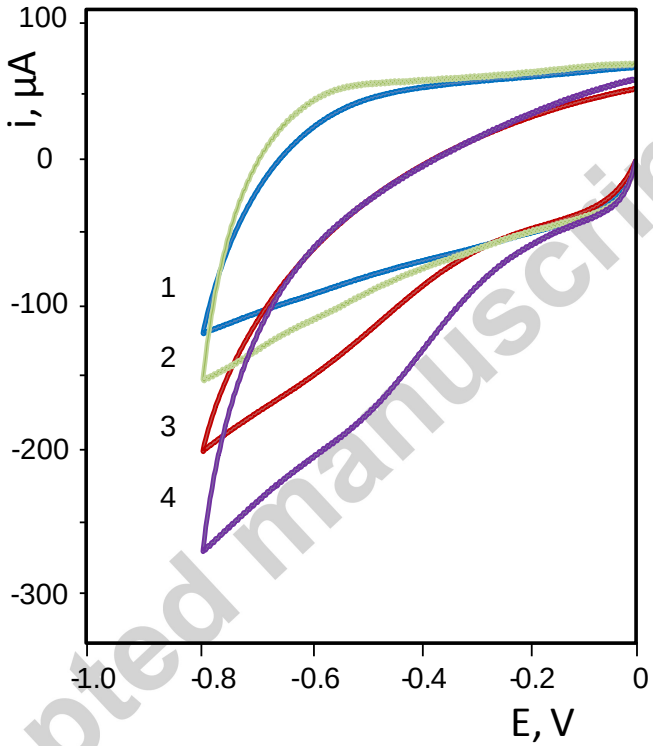

Figure 3. Cyclic voltammograms recorded in 0.1 M phosphate buffer solution (voltammograms 1 and 2) containing 0.044 mM H_2O_2 (voltammograms 3 and 4) at: (1) V-Phe-SWCNT/GCE (voltammograms 1 and 3) and V-Phe-SWCNT-HRP/GCE (voltammograms 2 and 4).

According with the cyclic voltammograms, a detection potential of – 0.3 V was selected for the amperometric measurements of H_2O_2 reduction and the subsequent determination of TGF-β1. Although the cathodic current increases as the potential is more negative, the

above value was chosen to avoid potential interferences from electroactive substances present in real samples.

The variables involved in the preparation of the immunosensor for TGF-β1 were optimized. The effect on the electrochemical responses of the following parameters were tested: a) the loadings of HRP and anti-TGF antibody onto V-Phe-SWCNT; b) the streptavidin loading onto SPCEs and c) the biotinylated antibody loading onto Strept-SPCEs. Other variables involved in the preparation of the modified electrodes such as the experimental conditions for grafting of SPCEs with 4-ABA diazonium salt or the amount of EDC/NHSS for covalent immobilization of biomolecules were optimized previously [Moreno-Guzmán et al., 2012]. Details on these optimization studies are provided in Supplementary Material and Figs. S6 and S7.

Analytical characteristics of the immunosensor.

Figure 4 shows the calibration plot for TGF-β1 constructed with the developed immunosensor under the optimized working conditions. Error bars were calculated from measurements carried out with three different immunosensors in each case. In addition, some typical recorded amperograms used for the construction of the calibration graph are also displayed. The steady state current vs. logarithm of TGF-β1 concentration follows the adjusted equation i, nA = (332 ± 9) log [TGF-β1], pg mL^{-1} - (99 ± 18) (r^2 = 0.996) with a range of linearity extending between 2.5 and 1000 pg mL^{-1} TGF-β1. This range covers almost three orders of magnitude and is adequate for the determination of the cytokine in clinical samples taking into account the expected concentrations, at ng mL^{-1} level, in plasma [Grainger et al., 2000]. The limit of detection, 0.95 pg mL^{-1}, was calculated according to the $3s_b$ criterion, where s_b was estimated as the standard deviation, expressed in

concentration units, of 10 blank current measurements (0 ng mL^{-1} TGF-β1). These analytical characteristics improve notably those reported with other previous immunosensors. For example, the lowest concentration in the calibration plot, 2.5 pg mL^{-1}, is six times lower and the limit of detection ten times lower than the corresponding values reported for immunosensors constructed using carboxylated magnetic beads [Sánchez-Tirado et al., 2017]. Moreover, the immunosensor described in this work provides a calibration plot covering a wider linear range of concentrations (extending up to almost an order of magnitude larger) with a slope 60 times higher and a slightly lower limit of detection than the values achieved with an immunosensor prepared through click chemistry [Sánchez-Tirado et al., 2016]. The developed immunosensor also exhibits a LOD value remarkably smaller than those provided with the aptasensor (1 ng mL^{-1}) [Matharu et al., 2014] and the impedimetric immunosensor (0.570 ng mL^{-1}) [Yao et al., 2016]. Most importantly, the analytical characteristics achieved with the proposed immunosensor also improve those claimed for the commercial ELISA kits. For example, Duo Sets ELISA Development System (DY240-05) from R&D Systems (www.rndsystems. com/products/human-tgf-beta-1-duoset-elisa_dy240) provides a calibration graph with a linear absorbance vs log [TGF-β1] ranging between 31 and 1000 pg mL^{-1}, and requires an assay time of 5h 20 min which is remarkably longer than the time needed for preparing and using the developed electrochemical immunosensor (2h 30 min). In both cases, the assay time was counted since the capture antibody was immobilized.

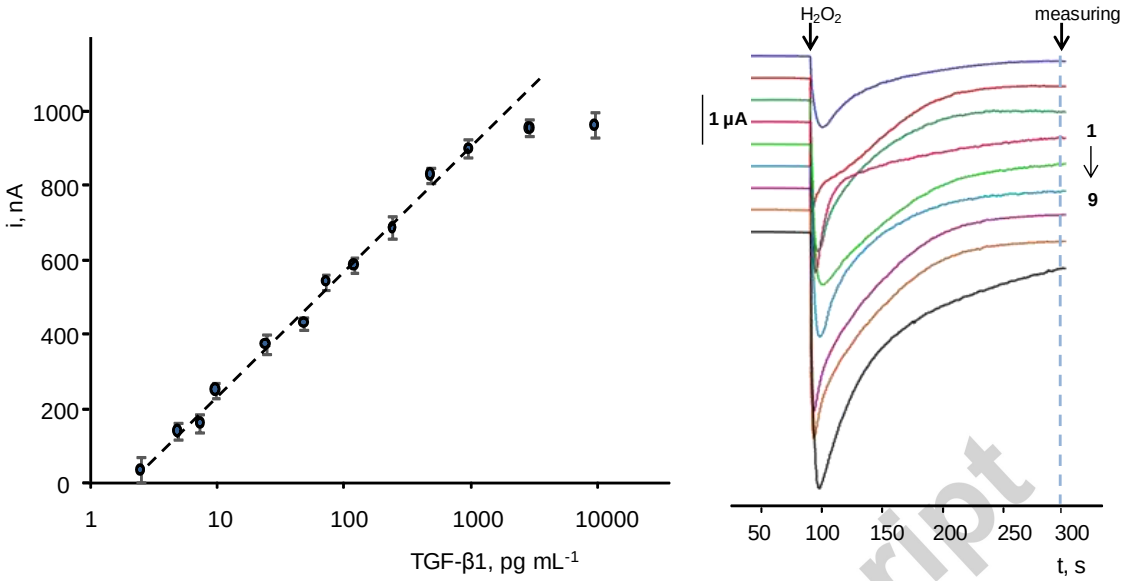

Figure 4. Calibration plot (left) and amperograms recorded (right) for the amperometric determination of TGF-β1 with the V-Phe-SWCNT(-HRP)-anti-TGF-TGF-β1- anti-TGF-Biotin-Strept/SPCE immunosensor; TGF-β1, μg mL^{-1}: 5 (1); 7.5 (2); 10 (3); 25 (4); 50 (5); 75 (6); 125 (7); 250 (8); 500 (9).

The reproducibility of the amperometric responses obtained with different immunosensors was evaluated by preparing sets of immunosensors both on the same day and on different days using a new anti-TGF-Biotin-Strept/SPCE in each case. Relative standard deviation (RSD) values of 3.4 % and 3.1 % (n=5) were calculated for the assays performed on the same day in the absence and in the presence of 125 pg/mL TGF-β1, respectively. In addition, RSD values of 6.5 % and 7.2 % (n=5) were obtained, respectively, for the measurements made on different days. These results reveal the good level of precision achieved in the fabrication and functioning of the developed immunosensor. Moreover, the storage ability of anti-TGF-Biotin-Strept/SPCE conjugates was also tested. Different anti-TGF-Biotin-Strept/SPCEs were prepared on the same day, stored under humidity

conditions at 4°C, and employed to prepare immunosensors to measure 125 pg mL^{-1} TGF-β1 on different days. The results obtained (not shown) indicated that the immunosensor responses remained within the control limits at ±3s, were s was the standard deviation of the measurements (n=10) carried out on the first working day, for at least 30 days (no longer storage times were tested) demonstrating the excellent stability of the anti-TGF-Biotin-Strept/SPCE conjugates. In addition, the stability of V-Phe-SWCNT(-HRP)-anti-TGF conjugates was also checked by measuring 125 pg mL^{-1} TGF- β1 on different days with immunosensors constructed with different V-Phe-SWCNT(-HRP)-anti-TGF conjugates prepared on the same day, and stored in phosphate buffer solution of pH 7.4, at 8°C. The immunosensor responses remained within the control limits at ± 3 s for at least 14 days.

A great selectivity against other proteins was also found. Figure 5 displays the immunosensor amperometric responses in the absence and in the presence of 50 pg mL^{-1} TGF-β1, and in the presence of 5 pg mL^{-1} adiponectin (APN), 50 ng mL^{-1} bovine serum albumin (BSA), 12 ng mL^{-1} cortisol, 50 ng mL^{-1} human immunoglobulin G (IgG), 50 pg mL^{-1} interleukin 1 beta (IL–1β), 50 pg mL^{-1} interleukin 6 (IL–6), 250 pg mL^{-1} interleukin 8 (IL–8), and 10 pg mL^{-1} tumoral necrosis factor alpha (TNF–α). These concentrations are those expected according to the literature in healthy individuals. As it is clearly seen in Figure 5, no significant interference was apparent for any potential interfering biomolecule. Interestingly, the moderate detection potential used (-300 mV) prevents the interference from electroactive species usually present in biological samples such as ascorbic (AA) and uric (UA) acids.

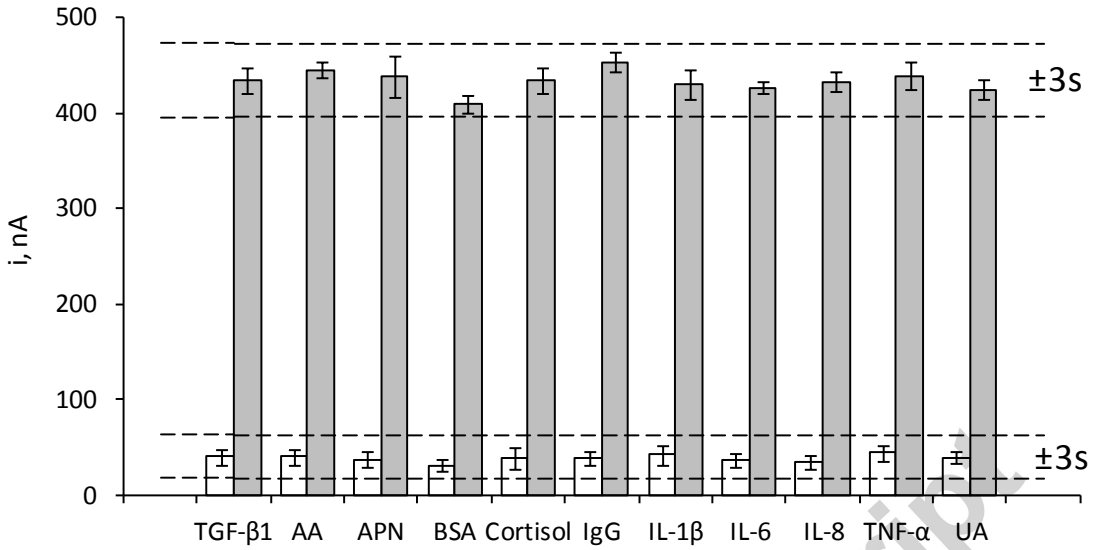

Figure 5. Amperometric responses measured with V-Phe-SWCNT(-HRP)-anti-TGF-TGF-β1-anti-TGF-Biotin-Strept/SPCE immunosensors for 0 (white) and 50 (grey) pg mL^{-1} TGF-β1 standards in the absence and in the presence of 370 μg mL^{-1} ascorbic acid (AA), 5 pg mL^{-1} adiponectin (APN), 50 ng mL^{-1} bovine serum albumin (BSA), 12 ng mL^{-1} cortisol, 50 ng mL^{-1} immunoglobulin G (IgG), 50 pg mL^{-1} interleukin 1 beta (IL-1β), 50 pg mL^{-1} interleukin 6 (IL-6), 250 pg mL^{-1} interleukin 8 (IL-8), 10 pg mL^{-1} tumoral necrosis factor alpha (TNF-α) and 50 μg mL^{-1} uric acid (UA).

Determination of TGF-β1 in saliva.

The usefulness of the immunosensor for the determination of low TGF-β1 concentrations in real samples was evaluated by analyzing saliva following the procedure described in section 2.3.5. Saliva from four volunteers were analyzed. Firstly, the possible existence of matrix effects was tested by comparing the slopes value of the calibration plot constructed by successive addition of aliquots of TGF-β1 standards to the sample with that measured with the calibration graph prepared with analyte standard solutions. The application of the

Student t test provided t_{exp} values 0.969, 0.615, 0.254 and 0.221 lower than the tabulated one, t_{tab} = 2.179 for α = 0.05 and n = 5. Therefore, the determination of TGF-β1 in saliva can be performed directly by interpolation of the amperometric current measured with the immunosensor for an aliquot of the undiluted sample, into the calibration plot constructed with standard solutions. The concentrations found in the analysis of the real samples (for two smoker and two non-smoker individuals) were compared with the results provided with a commercial ELISA kit (Table 1). As it can be seen, there is an excellent agreement between the results obtained by both methods. TGF-β1 concentration values of 24 pg mL^{-1} and 25 pg mL^{-1} TGF-β1 have been reported in the literature in saliva of healthy individuals [Yousefzadeh et al., 2006] [Brand et al., 2014]. Therefore, the values calculated with the immunosensor are also in good agreement with reported data. All these results demonstrated the usefulness of the developed immunosensor for the analysis of TGF-β1at low concentration levels in saliva with minimal sample treatment.

Table 1. Determination of TGF-β1 in real saliva samples

TGF–*β*1		
Saliva	**Immunosensor *(n = 5)*, pg/mL**	**ELISA *(n = 4)*, pg/mL**
smoker	27.6 ± 0.2	27.3 ± 0.2
smoker	26.4 ± 0.5	26.3 ± 0.1
non-smoker	21.2 ± 0.6	21.2 ± 0.1
non-smoker	22.8 ± 0.3	22.7 ± 0.5

4. Conclusions

Viologen-SWCNTs hybrids, prepared using a novel method by aryl-diazonium chemistry in the presence of isoamylnitrite followed by condensation of the resulting HOOC-Phe-SWCNT with 1-(3-aminoethyl)-4,4'-bipyridinium bromine and N-alkylation with 2-bromoethylamine, have been used as carrier tags for signal amplification in the construction of an amperometric immunosensor for TGF-β1. The implementation of a sandwich type immunoassay allowed improved analytical characteristic to be obtained in terms of wider linear dynamic range of response and lower detection limit than those reported with other previous immunosensors and those claimed for ELISA kits. In addition, a great selectivity against other proteins and ascorbic and uric acid was also found. The developed immunosensor was applied to the determination of TGF-β1 in saliva samples with minimal sample treatment and with results in excellent agreement with those obtained by using a commercial ELISA kit.

Acknowledgement

The financial support of projects CTQ2015-70023-R and CTQ2016-79189-R (Spanish Ministry of Economy and Competitivity Research Projects), S2013/MT-3029 (NANOAVANSENS Program from the Comunidad de Madrid) and PEII-2014-014-P (Junta de Comunidades de Castilla-La Mancha) are gratefully acknowledged.

Supplementary Material

1. Characterization of V-Phe-SWCNT hybrids: Fig S1 (TGA); Fig S2 (Raman); Fig S3 (FT-IR); Fig S4 (UV).
2. Characterization of V-Phe-SWCNT(-HRP)-anti-TGF: Fig S5A (UV); Fig S5B (FT-IR)

3. Optimization of the experimental variables involved in the preparation of the immunosensor; Fig S6 (effect of HRP and TGF concentration); Fig S7 (effect of the streptavidin and anti-TGF-Biotin loading. (PDF)

References

[Alvaro et al., 2005] Alvaro, M., Aprile, C., Atienzar, P., Garcia, H., 2005. J Phys. Chem. B, 109, 7692–7697.

[Brand et al., 2014] Brand, H.S., Ligtenberg, A.J.M., Veerman, E.C.I., 2014. Saliva and wound healing, in: ed. p. 56; Ligtenberg, A.J.M., Veerman, E.C.I. (Eds.) Saliva: Secretion and functions, Monogr. Oral Sci, Vol 24, Karger, Basel, p.56.

[Chen et al., 2009] Chen, G.P., Wang, X., Liu, A.-R., Quan, D.J. 2009. Mater. Sci. Eng. C, 29, 925–929.

[Conoci et al., 2014] Conoci, S., Mascali, A., Pappalardo, F., 2014. RSC Adv., 4, 2845–2850.

[Dong et al., 1997] Dong, S., Li, J., 1997. Bioelectrochem. Bioenerg., 42, 7-13.

[Gadgil et al., 2013] Gadgil, B., Damlin, P., Aaritalo, T., Kankare, J., Kvarnström, C., 2013. Electrochim. Acta, 97, 378–385.

[Ghica et al., 2005] Ghica, M. E., Brett, C.M.A., 2005. Anal. Chim. Acta. 532, 145–151.

[Gondram et al., 2010] Gondran, C., Orio, M., Rigal, D., Galland, B., Bouffier, L., Gulon, T., Cosnier, S., 2010. Electrochem. Commun.,12, 311–314.

[Grainger et al., 2000] Grainger, D.J., Mosedale, D.E., Metcalfe, J.C., 2000. 11, 133–145.

[Jia, 2008] Jia, J., 2008. Microchim. Acta, 163, 237–241.

[Kafi et al., 2007] Kafi, A.K.M., Lee, D.Y., Park, S.-H., Soo Kwon Y., 2007. Microchem. J., 85, 308–313.

[Kavosi et al., 2014] Kavosi, B., Hallaj, R., Teymourian, H., Salimi, A., 2014, Biosens. Bioelectron., 59, 389–396.

[Lee et al., 2016] Lee, D., Kim, Y.H., Park, S., 2016. J. Electrochem. Soc., 163, G93-G98.

[Liang et al., 2009] Liang, W., Yi, W., Li, S., Yuan, R., Chen, A., Chen, S., Xiang, G., Hu, C., 2009. Clin. Biochem. 42, 1524–1530.

[Liu et al., 2013] Liu, J., Chen, M., Qian, D.J., 2013. Colloids Surf., A, 436, 953–960.

[Matharu et al., 2014] Matharu, Z., Patel, D., Gao, Y., Haque, A., Zhou, Q., Revzin, A., 2014. Anal. Chem., 86, 8865–8872.

[Miodek et al., 2016] Miodek, A., Anh, H.Q., Sauriat-Dorizon, H., Korri-Youssoufi, H., 2016. Electroanalysis, 28, 1–10.

[Moreno-Guzmán et al., 2012] Moreno-Guzmán, M., Ojeda, I., Villalonga, R., González-Cortés, A., Yáñez-Sedeño, P., Pingarrón, J.M., 2012. Biosens. Bioelectron., 35, 82–86.

[Palacin et al., 2009] Palacin, T., Le Khanh, H., Jousselme, B., Jegou, P., Filoramo, A., Ehli, C., Guldi, D.; Campidelli, S., 2009. J. Am. Chem. Soc., 131, 15394–15402.

[Park et al., 2012] Park, J.H., Xue, H., Jung, J.K., Ryu, K., 2012. Korean J. Chem. Eng., 29, 1409–1412.

[Pfeiffer et al., 1996] Pfeiffer, A., Middelberg-Bisping, K., Drewes, C., Schatz, H., 1996. Diabetes Care, 19,1113-1117.

[Quan et al., 2010] Quan, D., Nagarale, R.K., Shina, W., 2010. Electroanalysis, 22, 2389–2398.

[Rahim Ruslinda et al., 2013] Rahim Ruslinda, A., Tanabe, K., Ibori, S., Wang, X., Kawarada, H., 2013. Biosens. Bioelectron., 40, 277–282.

[Sánchez-Tirado et al., 2017] Sánchez-Tirado, E., Martínez-García, G., González-Cortés, A., Yáñez-Sedeño, P., Pingarrón, J.M., 2017. Biosens. Bioelectron., 88, 9–14.

[Sánchez-Tirado et al., 2016] Sánchez-Tirado, E., González-Cortés, A., Yáñez-Sedeño, P., Pingarrón, J.M., 2016. Analyst, 141, 5730-5737.

[Straub et al., 2014] Straub, V., Gallego, A., de la Torre, G., Chamberlain, T.W., Khlobystov, A.N., Torres, T., Guldi, D.M., 2014. Faraday Discuss., 173, 233–256.

[Swetha et al., 2012] Swetha, P., Kumar, A.S., 2012. ECS Electrochem. Lett., 1, H1-H3.

[Tsapenko et al., 2013] Tsapenko, M.V., Nwoko, R.E., Borland, T.M., Voskoboev, N.V., Pflueger, A., Rule, A.D., Lieske, J.C., 2013. Clin. Biochem., 46, 1430–1435.

[Tuci et al., 2012] Tuci, G., Vinattieri, C.M., Luconi, L., Ceppatelli, M., Cicchi, S., Brandi, A., Filippi, J., Melucci, M., Giambastiani, G., 2012. Chem. Eur. J., 18, 8454–8463.

[Voggu et al., 2008] Voggu, R., Rout, C.S., Franklin, A.D., Fisher, T.S., Rao, C.N.R., 2008. J. Phys. Chem. C, 34, 13053–13056.

[Wang et al., 2008] Wang, X., Huang, H.X., Liu, A.R., Liu, B., Chen, M., Qian, D.J., 2008. Thin Solid Films, 516, 3244–3250.

[Wang et al., 2009] Wang, X., Liu, B., Chen, M., Qian, D., 2009. J. Nanosci. Nanotechnol., 9, 1441–1444.

[Wickenhauser et al., 1995] Wickenhauser, C., Hillienhof, A., Jungheim, K., Lorenzen, J., Ruskowski, H., Hansmann, M., Thiele, J., Fischer, R., 1995. Leukemia, 9, 310–315.

[Yao et al., 2016] Yao, Y., Bao, J., Lu, Y., Zhang, D., Luo, S., Cheng, X., Zhang, Q., Li, S., Liu, Q., 2016. Sens. Actuators B, 222, 127-132.

[Yousefzadeh et al., 2006] Yousefzadeh, G., Larijani, B., Mohammadirad, A., Heshmat, R., Dehghan, G., Rahimi, R., Abdollahi, M., 2006. Ann. NY Acad. Sci., 1091, 142–150.

Highlights

- Synthesis of viologen-SWCNT hybrids by aryl-diazonium chemistry.
- Preparation of TGF-β1 immunosensor by grafting with 4-carboxyphenyl onto screen-printed carbon electrodes.
- Signal amplification using V-Phe-SWCNT(-HRP)-anti-TGF as carrier nanotags.
- Application to real saliva samples.